Progress In Electromagnetics Research Letters, Vol. 106, 15–20, 2022

Metamaterial Perfect Absorber Using Vanadium Oxide Hexagonal Ring Structure

Mekala Ananda Reddy*, Namanathan Praveena, Nagarajan Gunavathi, and Ramasamy Pandeeswari

Abstract—A Metamaterial Terahertz perfect absorber is proposed in this letter. The structure comprises Vanadium oxide (VO_2) resonator hexagonal rings placed on top of a silicon dioxide (SiO_2) substrate in a concentric pattern on a metal ground layer, with 1 THz and 6 THz operating frequency. Numerical studies are done by an electromagnetic solver. The results show almost perfect absorption, with 112% average absorption at different incident polarization angles, in the range of 1.64 to 6.1 THz. The optimization is carried out on physical dimensions for maximum absorption results. The proposed design can be used as a highly efficient absorber in applications like solar energy harvesting, cloaking, sensing, imaging technology, and EMC projects.

1. INTRODUCTION

Terahertz technology has been influenced by the development in high-speed electronics and photonics [1–4]. The effort to solve accurate process information at terahertz frequencies in RF-photonics has been spurred. RF and optical waves often use dissimilar materials and device technologies. The optical technology offers wavelength parallelism, low energy consumption, and high bandwidth. Terahertz frequencies have very wide wireless applications in sensors [5, 6] and imaging. In the literature, metamaterial-based devices have been proposed, such as polarization converters, filters, and absorbers. Also, metamaterial absorber has many applications in stealth technology and imaging applications. Multiple resonant and multi-layer structures have been reported in order to achieve broadband absorption [7]. A dual-band metamaterial perfect absorber (MPA) for Ku band applications is reported in [8], hypersensitized metamaterials based on a corona-shaped resonator for efficient detection of glucose detailed in [9], and tunable left-hand characteristics in multi-nested square-split-ring enabled metamaterials reported in [10]. Vanadium dioxide (VO_2) changes from an insulator to a metal phase and significant change in conductivity at about 340 K. VO_2 is an effective and suitable candidate to achieve adjustable characteristics in the THz range [11–13].

This letter presents a Terahertz absorber consisting of three hexagonal vanadium dioxide rings, a silicon dioxide dielectric, and a metal ground layer. The absorption bandwidth is about 115% at 4 THz in the range of 1.64 to 6.10 THz. The conductivity of VO_2 changes from an insulating phase to a metallic phase, when it varies from 200 S/m to 2×10^5 S/m. The two absorption peaks in the electric field distribution are simulated and analyzed.

2. ANALYSIS AND DESIGN

The geometry of the Terahertz absorber is shown in Figure 1. It consists of three VO_2 hexagonal resonance rings, a dielectric, and a metal ground. The unit cell periodicity is $P = 30\,\mu$m. Figure 1(a)

Received 20 June 2022, Accepted 3 August 2022, Scheduled 17 August 2022
* Corresponding author: Mekala Ananda Reddy (anandareddy007@gmail.com).
The authors are with the Department of Electronics and Communication Engineering, NIT, Tiruchirapalli, India.

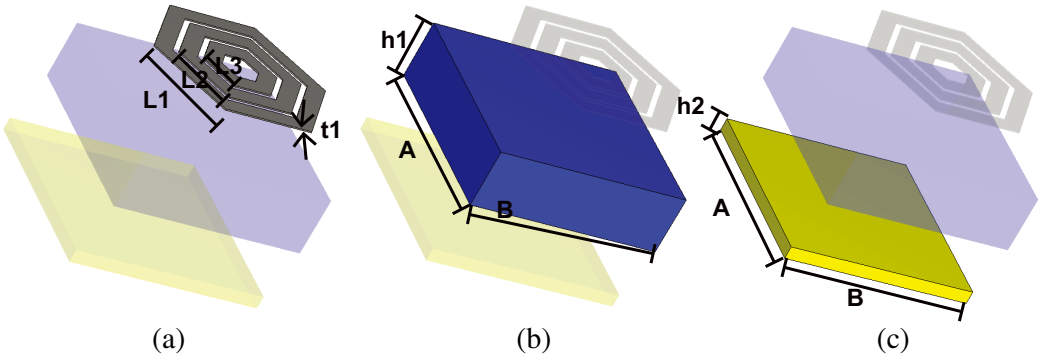

Figure 1. Geometry and dimensions of the THz metamaterial absorber. (a) Vanadium oxide (VO_2) hexagons. (b) Silicon dioxide (SiO_2) dielectric. (c) Metallic ground (Au). The parameter values are $L_1 = 14\,\mu m$, $L_2 = 10\,\mu m$, $L_3 = 6\,\mu m$, $h_1 = 9\,\mu m$, $h_2 = 2\,\mu m$, $t_1 = 0.2\,\mu m$, $A = 30\,\mu m$, $B = 30\,\mu m$.

shows three equally spaced hexagonal rings with side lengths $L_1 = 14\,\mu m$, $L_2 = 10\,\mu m$, and $L_3 = 6\,\mu m$, respectively. The thickness of VO_2 hexagonal ring $t = 0.2\,\mu m$. The optical characteristics of VO_2 in the Terahertz range are explained by the Drude model, which can be expressed as [14]

$$\varepsilon(\omega) = \varepsilon_\infty - \frac{\omega_p^2}{(\omega^2 + i\gamma\omega)} \tag{1}$$

where $\epsilon_\infty = 12$ is the high frequency dielectric permittivity, and $y = 0.75 \times 10^{13}\,rad/s$ is the collision frequency. The plasma frequency ω_p and conductivity σ can be expressed as

$$\omega_p^2(\sigma) = \frac{\sigma}{\sigma_0}\,\omega_p^2(\sigma_0) \tag{2}$$

The ground metal is gold having thickness $t = 2\,\mu m$ and conductivity $\sigma = 4.56 \times 10^7\,S/m$. The perfect matching layer (PML) boundary condition is set in the z-direction. The transmittance $T(\omega)$ is 0 when $t > \delta$ (skin depth). Hence, the absorptance $A(\omega)$ is expressed as

$$\mathrm{A}(\omega) = 1 - R(\omega) = 1 - |S_{11}(\omega)|^2 \tag{3}$$

where $S_{11}(\omega)$ is the reflection coefficient, and $R(\omega)$ is the reflectance.

3. RESULTS AND DISCUSSION

The absorption and reflection plots are shown in Figure 2. The absorption bandwidth is around 115% from 1.64 THz to 6.10 THz under normal incidence. Two absorption peaks are observed at 1.64 THz

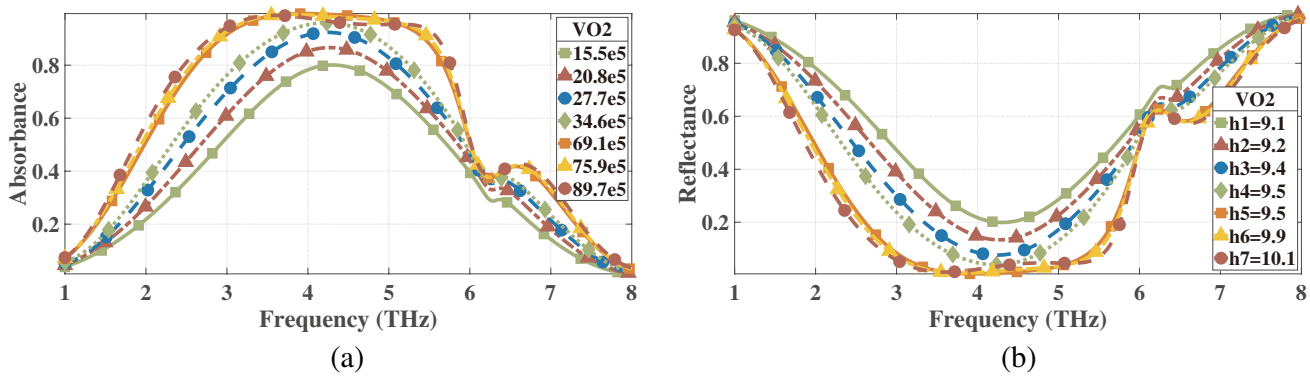

Figure 2. VO_2 with varying conductivity. (a) Absorbance. (b) Reflectance.

and 6.10 THz, respectively. The central frequency is 3.87 THz. It is observed from Figure 2(b) that the reflectance changes with varying conductivity (200 S/m to 2×10^5 S/m) accordingly. This is due to the change in VO_2 permittivity with the change in conductivity. The comparison of absorption between VO_2-based absorbers is presented in Table 1.

Table 1. Comparison of absorption between different VO_2 based absorbers.

References	Absorption	Percentage	Range
[15]	0.33	$> 90\%$	30%–100%
[16]	0.65	$> 90\%$	30%–98%
[17]	0.52	$> 90\%$	5%–100%
[18]	1.25	$> 90\%$	15%–96%
[19]	1.23	$> 90\%$	4%–100%
[20]	2.44	$> 90\%$	3.4%–100%
[21]	2.45	$> 90\%$	4%– 100%
Proposed Design	3.84	$> 115\%$	3%–100%

The absorption varying with the SiO_2 dielectric thickness is shown in Figure 3. The Reflectance (R) and Absorbance (A) are simulated and compared both in HFSS and CST software as shown in Figure 3(a). The dielectric thickness is 9 µm, i.e., $\approx$ 1/4 of the center wavelength satisfies the interference cancellation condition. The metamaterial absorber feasible processing steps include: (1) Plasma Enhanced Chemical Vapor Deposition (PECVD) process can be used to deposit 9 µm silicon dioxide film. (2) DC magnetron sputtering can be used to deposit the VOx onto the dielectric silicon dioxide film. (3) The photolithography process can be used to etch the surface of VO_2.

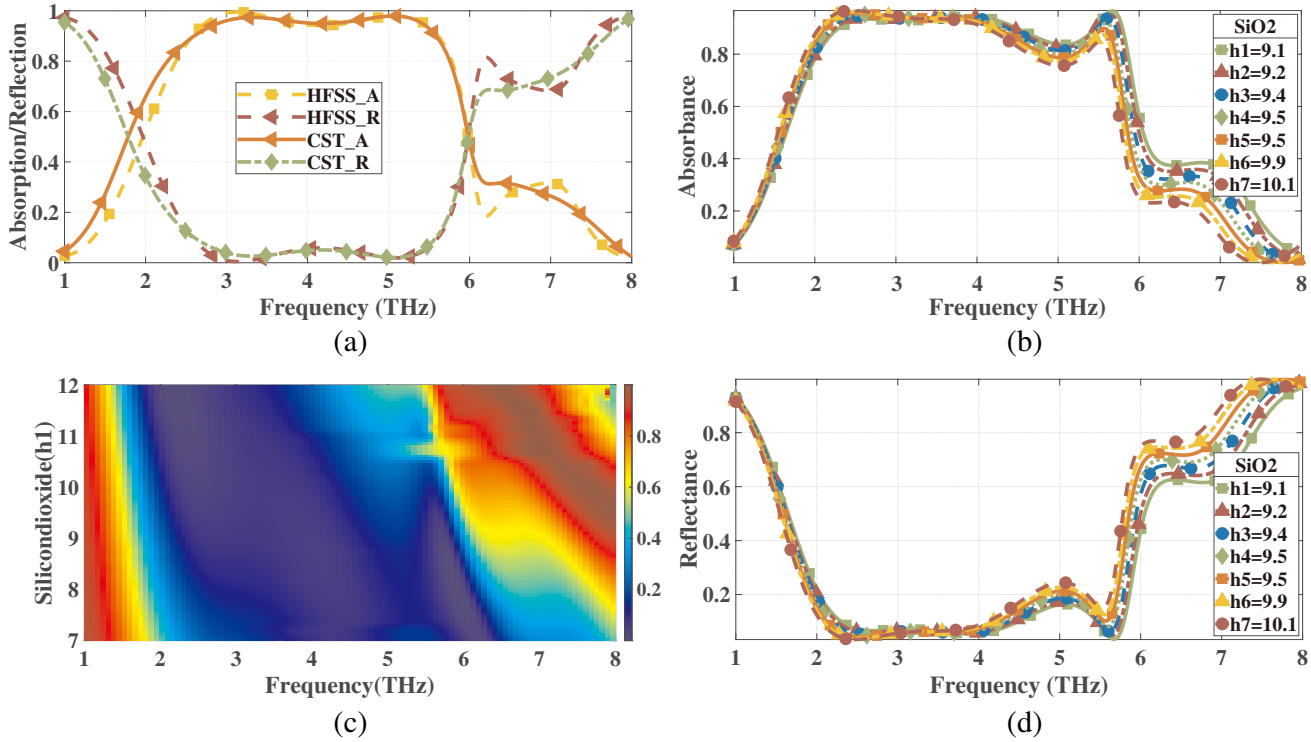

Figure 3. (a) Reflectance (R) vs Absorbance (A) simulation in HFSS and CST (b), (d) SiO_2 with varying dielectric thickness, (c) the colormap diagram of absorption spectrum of SiO_2.

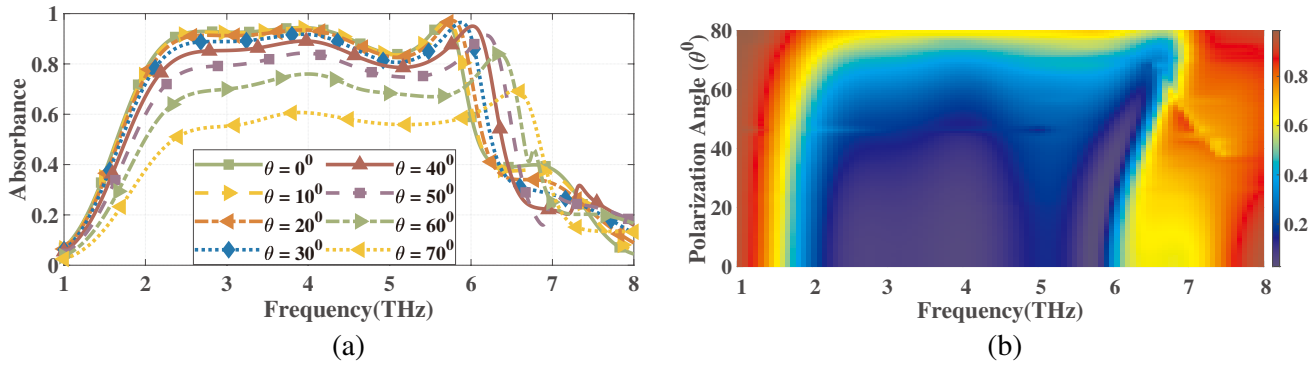

Figure 4. (a) Absorption plot with different incident angle (θ^0). (b) The colormap diagram of absorption spectrum of SiO_2.

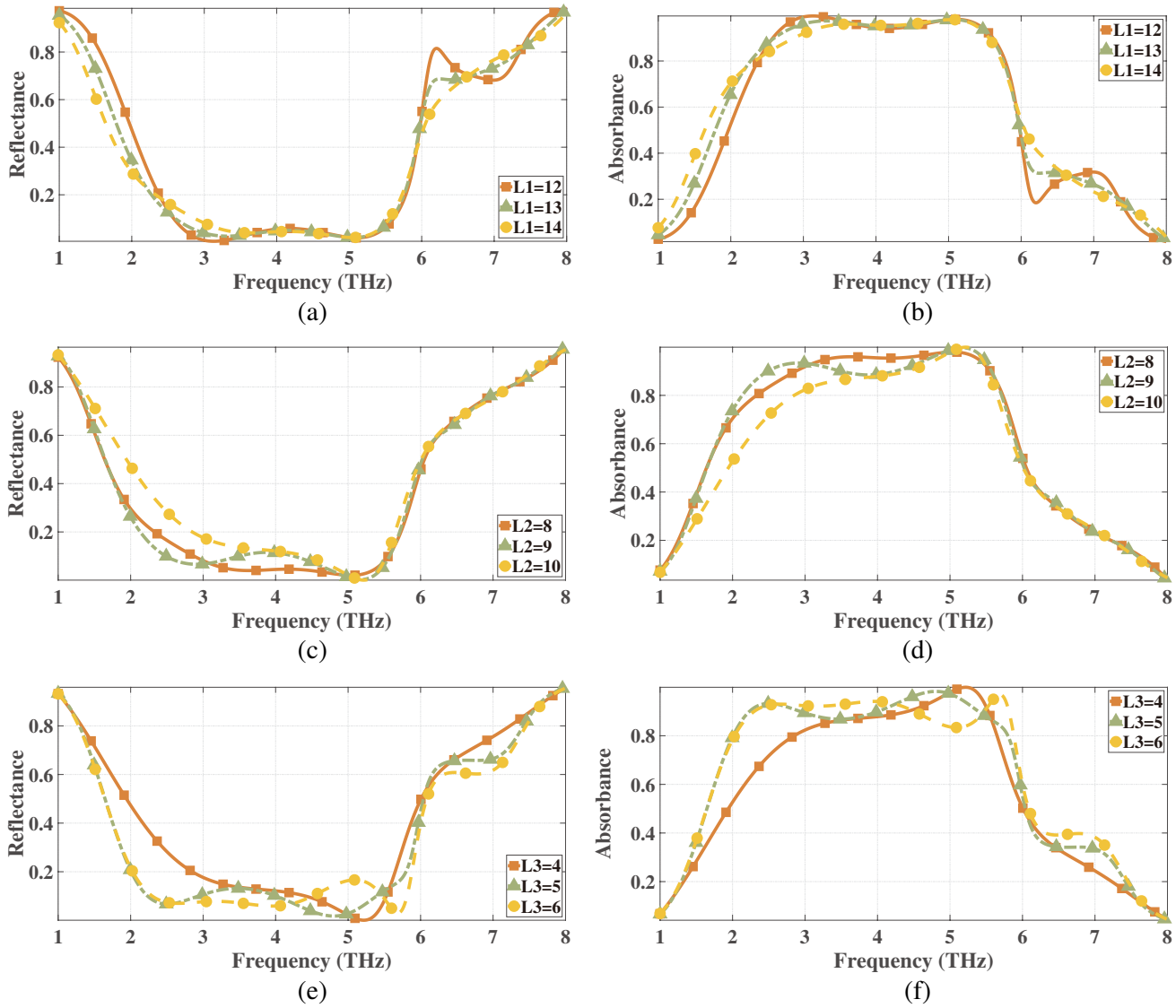

Figure 5. Parameter analysis by varying L_1, L_2, L_3. (a), (c), (e) Reflectance. (b), (d), (f) Absorbance.

The absorptions at different incident angles and the colormap diagram of polarization angles (θ^0) are plotted in Figure 4(a) and Figure 4(b), respectively. It is observed that the absorption decreases less than 60% as the incident angle increases more than 70°. The two absorption peaks of the electric field distributions are located at 1.64 THz and 6.10 THz and are shown in Figure 5. The magnetic coupling among the three hexagonal rings causes the maximum electric field distribution. Broadband absorption occurs when the absorber's two absorption peaks are widely separated. Thus, the multi-resonance hexagonal ring structure is useful for ultra-wideband absorbers. Figure 5 shows the parameter analysis of hexagonal ring side lengths L_1, L_2, and L_3. In Figure 5(b), the absorption bandwidth increases as the outer hexagonal side length L_1 increases, but the efficiency decreases due to the weak coupling effect between the outer and middle hexagonal rings. In Figure 5(d), the absorption bandwidth of the absorber increases as the width becomes wider, but the total absorption efficiency decreases. In Figure 5(f), the absorption efficiency increases as the size of the inner hexagonal ring side L_3 increases. It is observed from the above analysis that when the number of hexagonal rings increases, the absorption efficiency increases initially and then decreases. The maximum absorption efficiency is achieved when the hexagonal rings are three.

4. CONCLUSION

In this paper, an ultra-wideband THz absorber has been proposed. It consists of three VO_2 hexagonal rings, SiO_2 dielectric, and a metal ground layer. The results show 115% absorbance, and THz absorption bandwidth ranges from 1.64 THz to 6.10 THz with a center frequency of 3.87 THz under normal incidence. The conductivity of VO_2 changes from 200 S/m to 2×10^5 S/m with a difference in the temperature, which results in the absorption peak intensity adjusted continuously from 5% to 112%. The wave-interference theory and impedance matching theory can be used to verify perfect absorption. The absorption bandwidth has been optimized. The two absorption peaks' electric field distribution arises because of the coupling between adjacent rings. Also, the proposed absorber has polarization insensitivity and wide-angle absorption. The THz absorber can be used in many applications like modulators, sensors, solar energy harvesting, cloaking, sensing, imaging technology, and optic-electro switches.

REFERENCES

1. Heinz-Wilhelm, H., "Terahertz technology: Towards THz integrated photonics," *Nat. Photon.*, Vol. 4, 503–504, 2010.
2. Siegel, P. H., "Terahertz technology in biology and medicine," *IEEE Transactions on Microwave Theory and Techniques*, Vol. 52, No. 10, 2438–2447, 2004.
3. Jansen, C., S. Wietzke, O. Peters, M. Scheller, N. Vieweg, M. Salhi, N. Krumbholz, C. Jördens, T. Hochrein, and M. Koch, "Terahertz imaging: Applications and perspectives," *Applied Optics*, Vol. 49, No. 19, E48–E57, 2010.
4. Wanke, M. C., E. W. Young, C. D. Nordquist, M. J. Cich, A. D. Grine, C. T. Fuller, J. L. Reno, and M. Lee, "Monolithically integrated solid-state terahertz transceivers," *Nature Photonics*, Vol. 4, No. 8, 565–569, 2010.
5. Chen, T., D. Liang, and W. Jiang, "A tunable terahertz graphene metamaterial sensor based on dual polarized plasmon-induced transparency," *IEEE Sensors Journal*, 2022.
6. Cen, W., T. Lang, Z. Hong, J. Liu, M. Xiao, J. Zhang, and Z. Yu, "Ultrasensitive flexible terahertz plasmonic metasurface sensor based on bound states in the continuum," *IEEE Sensors Journal*, 2022.
7. Shan, Y., L. Chen, C. Shi, Z. Cheng, X. Zang, B. Xu, and Y. Zhu, "Ultrathin flexible dual band terahertz absorber," *Optics Communications*, Vol. 350, 63–70, 2015. [Online]. Available: https://www.sciencedirect.com/science/article/pii/S0030401815002734.

8. Al-Badri, K. S. L., Y. I. Abdulkarim, F. Özkan Alkurt, and M. Karaaslan, "Simulated and experimental verification of the microwave dual-band metamaterial perfect absorber based on square patch with a 450 diagonal slot structure," *Journal of Electromagnetic Waves and Applications*, Vol. 35, No. 11, 1541–1552, 2021. [Online]. Available: https://doi.org/10.1080/09205071.2021.1905560.
9. Abdulkarim, Y. I., F. F. Muhammadsharif, M. Bakır, H. N. Awl, M. Karaaslan, L. Deng, and S. Huang, "Hypersensitized metamaterials based on a corona-shaped resonator for efficient detection of glucose," *Applied Sciences*, Vol. 11, No. 1, 2021. [Online]. Available: https://www.mdpi.com/2076-3417/11/1/103.
10. Abdulkarim, Y. I., L.-W. Deng, J.-L. Yang, Ş. Çolak, M. Karaaslan, S.-X. Huang, L.-H. He, and H. Luo, "Tunable left-hand characteristics in multi-nested square-split-ring enabled metamaterials," *Journal of Central South University*, Vol. 27, No. 4, 1235–1246, Apr. 2020. [Online]. Available: https://doi.org/10.1007/s11771-020-4363-5.
11. Xu, Z. and Z. Song, "VO_2-based switchable metasurface with broadband photonic spin hall effect and absorption," *IEEE Photonics Journal*, Vol. 13, No. 4, 1–5, 2021.
12. Ren, Y. and B. Tang, "Switchable multi-functional VO_2-integrated metamaterial devices in the terahertz region," *Journal of Lightwave Technology*, Vol. 39, No. 18, 5864–5868, 2021.
13. Zhang, Y., P. Wu, Z. Zhou, X. Chen, Z. Yi, J. Zhu, T. Zhang, and H. Jile, "Study on temperature adjustable terahertz metamaterial absorber based on vanadium dioxide," *IEEE Access*, Vol. 8, 85154–85161, 2020.
14. Liu, M., H. Y. Hwang, H. Tao, A. C. Strikwerda, K. Fan, G. R. Keiser, A. J. Sternbach, K. G. West, S. Kittiwatanakul, J. Lu, S. A. Wolf, F. G. Omenetto, X. Zhang, K. A. Nelson, and R. D. Averitt, "Terahertz-field-induced insulator-to-metal transition in vanadium dioxide metamaterial," *Nature*, Vol. 487, No. 7407, 345–348, Jul. 2012. [Online]. Available: https://doi.org/10.1038/nature11231.
15. Song, Z., K. Wang, J. Li, and Q. H. Liu, "Broadband tunable terahertz absorber based on vanadium dioxide metamaterials," *Opt. Express*, Vol. 26, No. 6, 7148–7154, Mar. 2018. [Online]. Available: http://opg.optica.org/oe/abstract.cfm?URI=oe-26-6-7148.
16. Wang, S., C. Cai, M. You, F. Liu, M. Wu, S. Li, H. Bao, L. Kang, and D. H. Werner, "Vanadium dioxide based broadband THz metamaterial absorbers with high tunability: Simulation study," *Opt. Express*, Vol. 27, No. 14, 19436–19447, Jul. 2019. [Online]. Available: http://opg.optica.org/oe/abstract.cfm?URI=oe-27-14-19436.
17. Song, Z., M. Wei, Z. Wang, G. Cai, Y. Liu, and Y. Zhou, "Terahertz absorber with reconfigurable bandwidth based on isotropic vanadium dioxide metasurfaces," *IEEE Photonics Journal*, Vol. 11, No. 2, 1–7, 2019.
18. Bai, J., S. Zhang, F. Fan, S. Wang, X. Sun, Y. Miao, and S. Chang, "Tunable broadband THz absorber using vanadium dioxide metamaterials," *Optics Communications*, Vol. 452, 292–295, 2019. [Online]. Available: https://www.sciencedirect.com/science/article/pii/S0030401819306492.
19. Dao, R.-N., X.-R. Kong, H.-F. Zhang, and X.-R. Su, "A tunable broadband terahertz metamaterial absorber based on the vanadium dioxide," *Optik*, Vol. 180, 619–625, 2019. [Online]. Available: https://www.sciencedirect.com/science/article/pii/S0030402618319284.
20. Song, Z., M. Jiang, Y. Deng, and A. Chen, "Wide-angle absorber with tunable intensity and bandwidth realized by a terahertz phase change material," *Optics Communications*, Vol. 464, 125494, 2020. [Online]. Available: https://www.sciencedirect.com/science/article/pii/S0030401820301346.
21. Huang, J., J. Li, Y. Yang, J. Li, J. li, Y. Zhang, and J. Yao, "Active controllable dual broadband terahertz absorber based on hybrid metamaterials with vanadium dioxide," *Opt. Express*, Vol. 28, No. 5, 7018–7027, Mar. 2020. [Online]. Available: http://opg.optica.org/oe/abstract.cfm?URI=oe-28-5-7018.